Polymer Bulletin 56, 413–426 (2006)
DOI 10.1007/s00289-006-0506-6

Polymer Bulletin

Structure and thermal properties of titanium dioxide-polyacrylate nanocomposites

Wan tao[1,2], Feng fei[1], Wang yue-chuan[1] (✉)

1: College of polymer science and engineering, State Key Laboratory of Polymer Materials Engineering, Sichuan University, Chengdu, China, 610065
2: College of materials and bioengineering, Chengdu University of Technology, Chengdu, China, 610059
E-mail: wantaos@sohu.com; gycwang@163.net

Received: 28 July 2005 / Revised version: 28 October 2005 / Accepted: 9 January 2006
Published online: 27 January 2006 –

Summary

UV curable, transparent acrylic resin/titania organic–inorganic hybrid films were prepared by controlled hydrolysis of titanium tetrabutoxide (TTB) in Span85/Tweeen80 reverse micelles and subsequent in situ photopolymerization of acrylic monomers. The qualitative content of TiOTi group and TiOH was monitored by FTIR spectrum, and the thermal stability and film surface were characterized by TGA, DSC and AFM, respectively. TGA data show that TiO_2-hybrid films can upgrade the decomposition onset temperature and the temperature at which there is a maximum mass loss rate (T_{max}). DSC data show that prolonged exposure to UV light and post-thermal treatment can decrease the T_{onset} and T_{peak} of the exothermal peak and the condensation temperature between TiOH, and increase $\triangle H$ of the exothermal peak. FTIR spectra show the presence of two $\nu s(COO^-)$ modes with the νa-νs splitting magnitude($\triangle \nu$ $\sim$87cm^{-1} and 148cm^{-1},respectively), suggesting that acrylic acid acts as a bidentate coordination mode and therefore chemical linkages exist between inorganic and organic phases. AFM phase images showed the presence of inorganic domains, with mean size of 21.6nm -28.8nm, were uniformly dispersed in the polymeric networks.

Keywords: photopolymerization; titanium dioxide; nanocomposites

1. Introduction

As novel functional materials, hybrid organic–inorganic nanocomposites offer the opportunity to combine the desirable properties of organic polymers (toughness, elasticity) with those of inorganic solids (hardness, chemical resistance). Since the materials have been largely applied in many areas such as optics, electronics, ionics, mechanics, protective coatings, catalysis, sensors, and biology [1-5], they have received much attention in the fields of material science.

The major driving forces behind the intense activities in this area are the new and different properties of the nanocomposites which the traditional macroscale composites

and conventional materials do not have. For example, unlike the traditional composite materials which have macroscale domain size of millimeter and even micrometer scale, most of the organic/inorganic hybrid materials are nanoscopic, with the physical constraint of several nanometers, typically 1-100 nm. Therefore, they are often still optically transparent materials although microphase separation may exist.

Up to now, there are only very few literatures reporting the preparation of polymer/titania hybrid materials by the sol-gel method although titania has unique mechanical, thermal, optical and electronic properties [6,7]. Wilkes et al. [8] successfully prepared the high refractive index organic–inorganic hybrid materials by using titanium tetraisopropoxide as the inorganic precursor to react with triethoxysilane-capped poly (arylene ether ketone) and poly (arylene ether sulfone). Lee and Chen [9] had synthesized the high-refractive index PMMA–titania hybrid thin films, which could potentially be used as optical thin films. Hiroyo et al[10] successfully prepared the photosensitive inorganic–organic hybrid films from the titanium alkoxide containing vinylpyrrolidone (VP) and the hybrid film has excellent patternability and controlled refractive index in the range between 1.8 and 2.1 after post-thermal treatment between 150°C-400°C.

Our approach differs from the above-mentioned approaches to realize inorganic-organic nanocomposites in that it is sol-gel process in reverse micelles and subsequent in-situ photopolymerization, using reactive monomer as continuous oil phase without the extraction of the synthesized nanoparticles from the transparent solution. So this research opens up a new kind of nanocomposite synthesis method, which can be applied to other inorganic-organic nanocomposites besides titania/polymer nanocomposites.

This study is the first to investigate the formation of transparent titania/polyacrylate nanocomposites via hydrolysis of titanium tetrabutoxide (TTB) in Span80/Tween80 reverse micelles and entrapment of nanosized titania particles by subsequent photopolymerization. The structures of the hybrid films were investigated by atomic force microscopy (AFM) and FTIR, as well as the thermal stability by TGA and DSC. Transparent hybrid films with tuneable refractive index of 1.46-1.52 and small shrinkage, can be potentially used as holographic recording materials.

2. Experimental

2.1 Materials

Butyl acrylate (BA), chemical grade, washed with 30wt% NaOH solution three times. Acrylic acid (AA), analytical grade, used without further purification. Sorbite anhydride monostearic acid ester (Span-85) and Tween 80 (polyoxyethylene sorbitan monooleate), commercial grade, Beijing Chemical Co. Titanium tetrabutoxide (TTB), Darocur1173 (2-hydroxy-2-methylpropiophenone), and trimethylolpropyltriacrylate (TMPTA), chemical grade, used without further treatment.

2.2 Preparation of titania reverse micelles

Titania reversed micelles were synthesized with titanium tetrabutoxide (TTB) as precursor alkoxide, Span-85 and Tween 80 as surfactants, butyl acrylate(BA) as reactive solvent ,acrylic acid(AA) as carboxylic acid ligand , trimethylolpropyl triacrylate (TMPTA) as crosslinker and distilled water for hydrolysis. Span-85 and

Tween 80 were first mixed in butyl acrylate and then water was added dropwise to form transparent reverse micelles. Mixtures of acrylic acid and TTB were added carefully into the above reverse micelles while the solution is stirred mildly. After hydrolysis of titanium butoxide at room temperature for at least 30min, stable and clear titania reversed micelles were successfully obtained and used for the preparation of the hybrid films. The mass ratio was BA: TMPTA: surfactant: H_2O:TTB:AA= 100:10:10:4.5:30:15.

2.3 Preparation of titania-acrylic polymer hybrid films

The curing of the hybrid films was induced using UV irradiation. For that purpose, a photoinitiator 2-hydroxy-2-methylpropiophenone (5wt%, based on the total monomer weight) was added to the formulations. Hybrid organic–inorganic films were deposited via casting on pre-cleaned soda-lime glass substrates. Photopolymerization was achieved by irradiate the samples with a 50 $mW.cm^{-2}$ high pressure mercury lamp. After about 6min irradiation, the transparent hybrid films were obtained.

2.4 Characterizations

DSC of the hybrid film was measured on Perkin-Elmer DSC-7 instrument. The temperature program was 10.0 K/min from 0°C to 250°C, and the amount of sample was about 5～15mg under N_2 atmosphere. TGA of the hybrid film was measured on a Dupont 2100 instrument. The temperature program was 10.0 K/min from 20°C to 200°C, and the amount of sample was about 48～60mg under N_2 atmosphere. Film surface morphologies were examined by AFM measurements using a Digital Instruments NanoScope IIIa instrument in tapping mode using silicon tips with cantilever driving amplitudes of 45-80 nm and feedback achieved at about 60% of the driving amplitude. Infrared spectra were taken with a 510 Nicolet FTIR spectrometer.

3. Results and discussion

3.1 Preparation of titania-acrylic polymer hybrid films

The sol -gel process is a powerful method for the design of new materials based on the hydrolysis and condensation reactions of molecular precursors such as metal alkoxides. In the case of TTB, the overall hydrolysis and condensation reaction are described as

$$Ti(OR)_4 + xH_2O \longrightarrow Ti(OH)_x(OR)_{4-x} + xROH \quad (1)$$

$$(OR)_{4-x}(OH)_{x-1}Ti\text{-}OH + XO\text{-}Ti(OH)_x(OR)_{3-x} \longrightarrow (OR)_{4-x}(OH)_{x-1}Ti\text{-}O\text{-}Ti(OR)_{3-x}(OH)_x + XOH \quad (2)$$

where R= $-(CH_2)_3CH_3$; X=H,R

However, the precursor titanium tetrabutoxide is very reactive and direct hydrolysis usually leads to precipitates. For these systems, direct precipitation can be avoided by addition of hydroxylated complexing ligands to the titanium precursor [11] or by confinement of water in reverse micelles [12-14]. In the reverse micellar solution(as demonstrated in Fig 1), hydrolysis may occur inside the reverse micelle by penetration of the Ti precursor through the surfactant layer, or in the hydrocarbon phase by reaction with water attached to the polar head of a surfactant molecule released from the reverse micelle. Condensation reactions lead to the formation

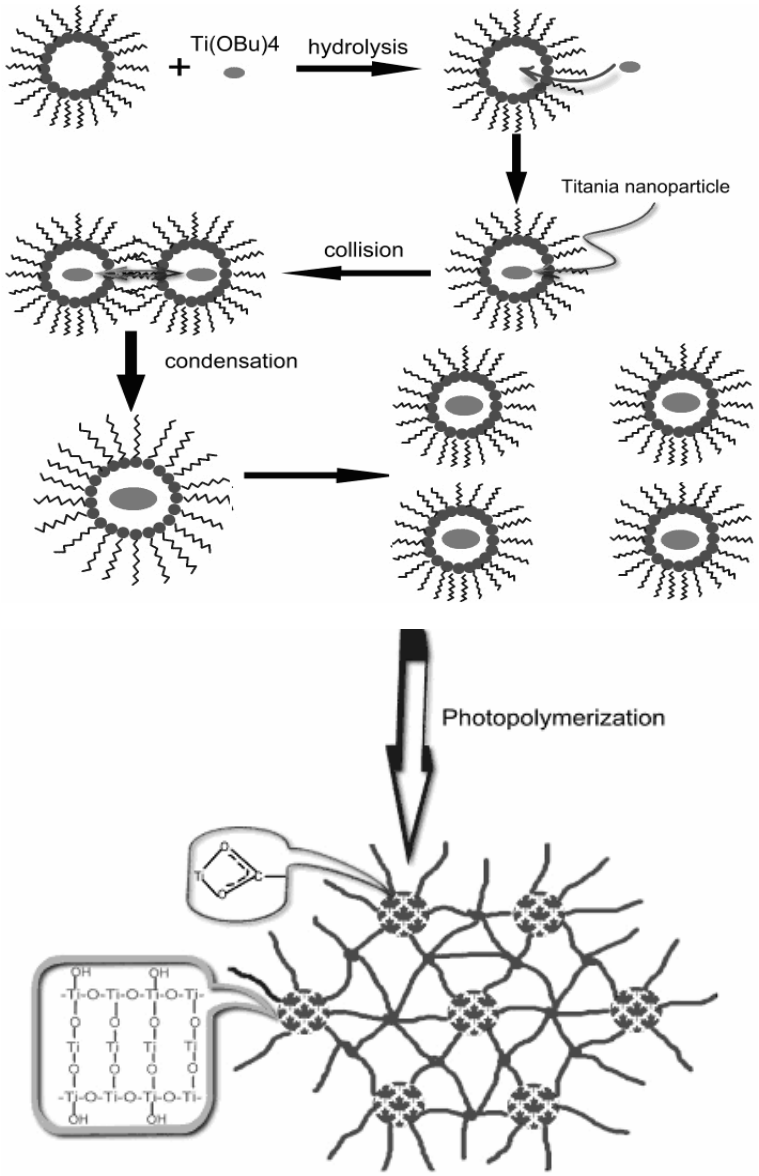

Fig 1 Schematic illustration of the preparation of titania/acrylic polymer nanocomposites

Ti-O-Ti bridges and particle growth. These particles are partially hydroxylated, and condensation reactions between them give precipitates or generate a network enclosing the liquid phase. Both processes involve the rearrangement of surfactant molecules that may be either adsorbed to the partially hydroxylated skeleton or forming reverse micelles in the solution phase. Therefore, the hydrolysis and condensation reactions were controlled by confinement of titania nanoparticles inside reverse micelles.

Titanium alkoxides are, in fact, known to readily react with carboxylic acids such as MAA[15-17] in mild conditions by competitive pathways: substitution (Eq 3), non-hydrolytic condensation and/ or elimination of an ester (Eq 4) that generates Ti-O-Ti bonds, or by hydrolysis-condensation (Eq 1 and 2) after a slow esterification (Eq 4).

$$Ti(OR)_4 + xR'COOH \longrightarrow Ti(OR)_{4-x}(R'COO)_x + xROH \quad (3)$$

$$n\ Ti(OR)_{4-x}(R'COO)_x \longrightarrow n/2[(OR)_{3-x}Ti\text{-}O\text{-}Ti(RCOO)_{x-1}] + R'COOR \quad (4)$$

$$ROH + R'COOH \longrightarrow R'COOR + H_2O \quad (5)$$

PERRIN[18] prepared the organic/inorganic hybrids from titanium butoxide and methyl methacrylate (MMA)-*n*-butyl methacrylate (*n*-BMA)-methacrylic acid (MA) terpolymers via the sol-gel process. Firstly, a terpolymer solution in toluene was added dropwise to $Ti(OBu)_4$ under vigorous stirring and a homogeneous and stable solution was successfully obtained. Drying of these solutions give semi-transparent hybrid materials. The interactions between the acid groups of the polymer and titanium butoxide were investigated by FT-IR spectroscopy and the terpolymer is found to be bonded to titanium through chelating carboxylate ligands. In this study reactive monomer acrylic acid (AA) was used as carboxylic acid ligand to further control the hydrolysis reaction and construct the chemical linkages between the organic and inorganic phases.

After the formation of stable and transparent titania reverse micelles, a photo-initiator was added and the mixtures were applied to high pressure mercury lamp to irradiate for 6min, and finally the titania-acrylic polymer hybrid films were formed.

3.2 Thermal stability study

The thermal stability of the titania-acrylic polymer hybrid film is evaluated using the TGA technique at programmed heating process (10°C/min). The results are shown in Fig. 2 and Table 1. From the differential curves of TGA the temperature at which there is a maximum mass loss rate(T_{max}), as well as the decomposition onset temperature(T_{onset}), is considered a parameter for the estimation of the thermal stability.

As shown in Fig1 and Table1, sample A (pure polyacrylates) exhibits a gradual mass loss starting from ambient temperature to 317.7°C, accompanied by a mass loss of 4.92% and a DTGA of 1.84%/min. This can be mainly attributed to the removal of volatile unreacted monomers, and then it shows an almost complete mass loss about 97.03% and a DTGA of 4.08%/min up to 413.2°C.

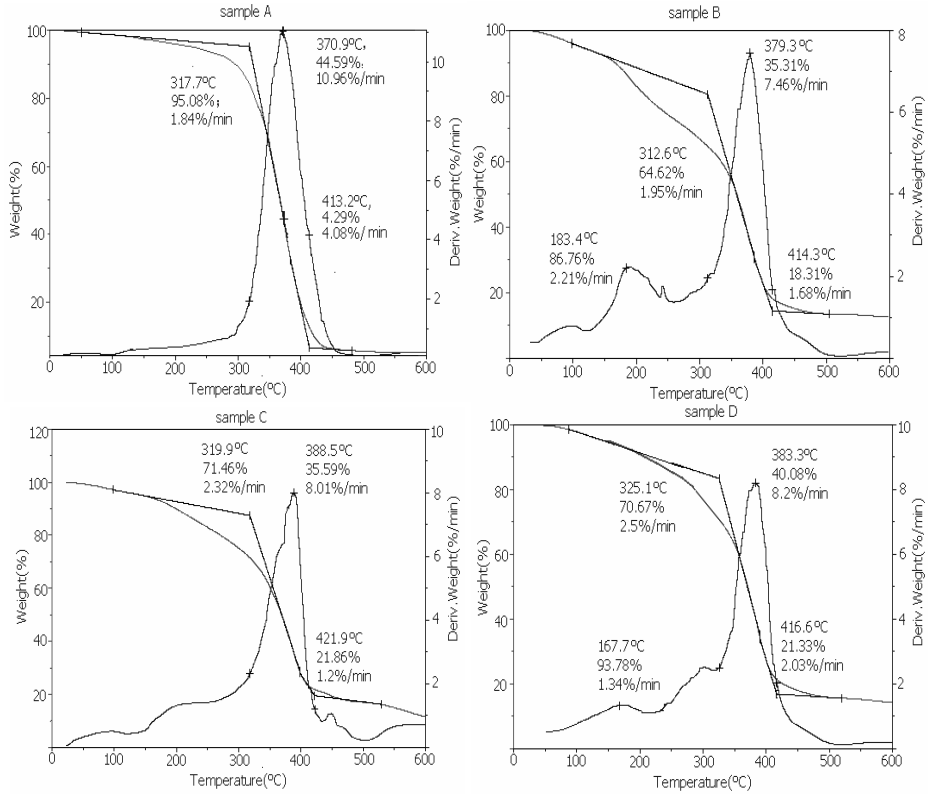

Fig 2 TGA and DTGA curves of the hybrid films as a function of irradiation and post-thermal treatment
Sample A: TTB=0wt%, pure polyacrylates without surfactant and water
Sample B: TTB=30wt%, room temperature, photocuring 6min
Sample C: TTB=30wt%, 90 °C 80h, photocuring 6min
Sample D: TTB=30wt%, photocuring 1h

Table 1 The TGA and DTGA data of the TiO_2-PBA hybrid films

samples	T_{onset}(°C)	T_{max}(°C)	Residue(%)at T_{max}	DTGA(%/min) at T_{max}
A	317.7	370.9	44.6	11.0
B	312.5	379.3	35.3	7.5
C	317.9	388.5	35.6	8.0
D	325.1	383.3	40.1	8.2

Sample A: TTB=0wt%, pure polyacrylates without surfactant and water
Sample B: TTB=30wt%, room temperature, photocuring 6min
Sample C: TTB=30wt%, 90 °C 80h, photocuring 6min
Sample D: TTB=30wt%, photocuring 1h

On the contrary, Sample B without post-thermal treatment shows a $DTGA_{max}$ at 183.4°C between 133.0°C and 255.1°C, with a corresponding mass loss between 4.28% and 26.47%. This corresponds to the removal of unreacted monomers,

surfactants, 1-butanol and absorbed water in the hybrid films. However, there is little mass loss above 500°C, indicative of an almost complete decomposition of organic molecules, and stabilization of TiO_2 in the hybrid film.

It is noteworthy that an enhanced thermal stability of the hybrid films can be achieved by way of post-thermal treatment and prolonged exposure to UV light. As compared with that of sample A, T_{onset} of sample C and sample D, increase from 317.7°C to 319.9°C and 325.1°C, and T_{max} of sample C and sample D increase from 370.9°C to 388.5°C and 383.3°C, respectively.

Except for the hybrid films without post-thermal treatment all the other titania-acrylic polymer hybrid materials have an enhanced decomposition onset temperature, as compared to sample A. As shown in Table 1, T_{onset} of organic polymer of sample B (312.5°C) is a bit lower than that of sample A (317.7°C). This can be ascribed to the removal of water and 1-butanol released from the hydrolysis of TTB, resulting in a larger slope of the TGA curve of sample B within the initial temperature than that of sample A without water and 1-butanol removal.

Obviously the titania-acrylic hybrid films can upgrade T_{onset} and T_{max}. This is due to that the inorganic materials in the polymer matrix can act as a superior insulator and mass transport barrier to the volatile molecules generated during decomposition.

In addition to the thermal stability shown by TGA, the TiO_2 particle content can be estimated by TGA at temperature as high as 600°C, at which all organic molecules have almost completely decomposed, supported by the fact that the samples shows little weight loss upon heating up to 600°C under nitrogen atmosphere(the residue of the organic molecules of Sample A is 2.57wt% at 600°C). As shown in Table 2, the TiO_2 content calculated from the reactant stoichiometry and found by TGA experiments are in poor agreement. The difference between the calculated and measured TiO_2 amount from TGA was ascribed to the presence of residual TiOH at 600°C.

Table 2 Compositions of the nanosized titania/polyacrylate hybrid films after removal of the organic molecules

	samples	B	C	D
TiO_2	cacl	8.15	8.15	8.15
content (%)	Found	9.67	9.61	9.57

Sample B: TTB=30wt%, room temperature, photocuring 6min
Sample C: TTB=30wt%, 90 °C 80h, photocuring 6min
Sample D: TTB=30wt%, photocuring 1h

DSC curves of titania-acrylic polymer hybrid films were shown in Fig 3 and Table 3. DSC curves have one endothermic peak and one exothermic peak in the temperature range of room temperature and 300°C for all the samples except for the sample A (TTB=0wt %). The first peak at 120-200°C, an endothermic process, is due to the volatilization of some organic materials, such as unreacted monomers, absorbed water and surfactant as well as 1-butanol released from the hydrolysis reaction; the second peak, an exothermal process, localized between 230-280°C, is evidently caused by the condensation between the residual TiOH at the TiO_2 surface[19,20].

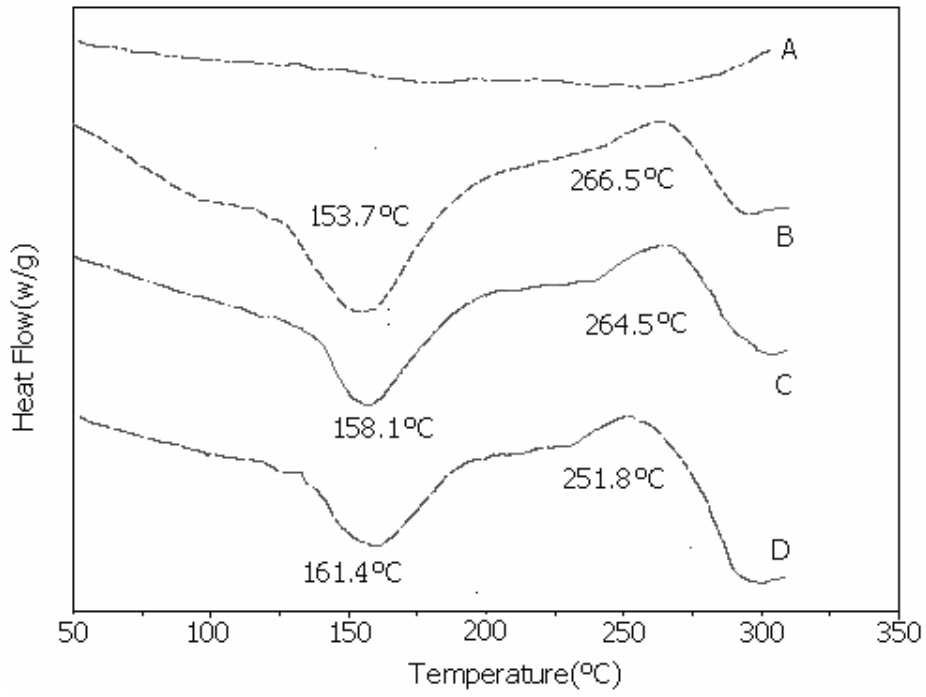

Fig 3 DSC curve of the nanosized titania –PBA hybrid films
Sample A: TTB=0wt%, photocuring 6min
Sample B: TTB=30wt%, room temperature, photocuring 6min
Sample C: TTB=30wt%, 90 °C 80h, photocuring 6minSample D: TTB=30wt%, photocuring 1h

Table 3 The DSC data of the nanosized titania –acrylic polymer hybrid films

Samples	First peak			Second peak		
	T_{onset}, °C	T_{peak},°C	△H,J/g	T_{onset}, °C	T_{peak}, °C	△H,J/g
B	123.3	153.7	28.08	242.9	266.5	8.519
C	137.5	158.1	19.24	239.1	264.5	11.72
D	137.8	161.4	18.47	237.1	251.8	13.44

Sample B: TTB=30wt%, room temperature, photocuring 6min
Sample C: TTB=30wt%, 90 °C 80h, photocuring 6min
Sample D: TTB=30wt%, photocuring 1h

For sample B without post-thermal treatment, an endothermal peak appeared on the DSC curve, with T_{onset} at 123.3°C and T_{peak} at 153.7°C as well as △H of 28.1J/g; However, for sample C with post-heat treatment 80h at 90°C, the T_{onset} and T_{peak} of the endothermal peak increased from 123.3°C to 137.5°C and 153.7°C to 158.1°C, respectively, accompanied by an corresponding decrease of △H from 28.08 J/g to 19.24 J/g. For sample C, post-thermal treatment can favor the formation of dense inorganic networks, further restrain the movement of some volatile organic molecules, and therefore enhance the T_{onset} and T_{peak} of the endothermal process.

It is noteworthy that exposure to UV light has much more significant effect on the T_{onset} and T_{peak} of the endothermal process than that of post-thermal treatment. As

shown in Table 3, T_{onset} and T_{peak} of the endothermal peak of sample D, is a bit higher than that of sample C. Exposure to UV light can accelerate the dehydration of TiOH by condensation [21, 22], thus increase the density of inorganic networks, constrain the mobility of organic molecules and increase the T_{onset} and T_{peak} of the endothermal peak.

For the second peak, an exothermal process, as shown in Table 3, exposure to UV light and post-thermal treatment can decrease the T_{onset} and T_{peak} and increase the $\triangle$H of the exothermal peak, as compared with that of sample B. This indicates that exposure to UV light and post-thermal treatment can decrease the condensation temperature between TiOH and increase the condensation enthalpy. This may be attributed to that exposure to UV light and post-thermal treatment can favor the formation of dense inorganic networks and make the hydrolyzed groups adjacent each other, and therefore decrease the reaction temperature.

3.3 FTIR study

The FTIR spectra of the hybrid films with different photocuring time and post-thermal treatment are shown in Fig 4. All of the samples show major absorption band associated with acrylic polymer, such as the symmetrical and asymmetrical CH_3 , $-CH_2-$ stretching at 2872, 2853 and 2965, 2928cm^{-1} respectively; The characteristic bands at 1735cm^{-1} and 1633cm^{-1} can be attributed to the C=O stretching, and associated water and unreacted monomer, respectively; the C-O stretching vibration is designated at 1100～1200cm^{-1}; In the high wave number spectral range a broad band between 3600 and 3100 cm^{-1} was assigned to fundamental stretching vibration of different O H hydroxyl groups (free or bounded). In the low wave number spectral range a not very sharp peak at ～948cm^{-1} assigned to TiOH species produced from incomplete condensation[23, 24]. Finally in the range 650–400 cm^{-1} we find a broad band with one peak of 485cm^{-1} that is assigned to Ti-O-Ti stretching vibration[25]. In this paper we will focus on the band around 948 and 485 cm^{-1} to calculate the relative content of TiO_2.

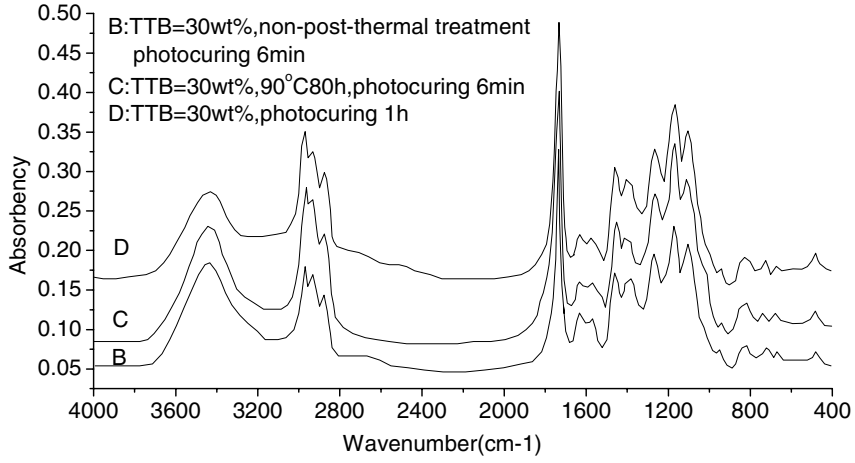

Fig 4 FTIR spetrum of the hybrid film as a function of photocuring time and thermal treatment

Upon photopolymerization and thermal treatment, the intensity of the stretching absorption of C=O at 1735cm^{-1} should not be affected. Hence, the relative intensity of TiOH(948cm^{-1}),Ti-O-Ti band(485cm^{-1}) to $\nu_{C=O}$ (at 1735cm^{-1}) can be used qualitatively to evaluate the extent of the hydrolysis and condensation, and the relative content of OH, TiOTi, and TiOH are summarized in Table 4.

Table 4 TiOH and Ti-O-Ti relative content as a function of thermal treatment and photocuring time

	samples	B	C	D
Internal standard ($\nu_{C=O}$ at 1735cm^{-1})	$A_{\nu(OH)}/ A_{\nu C=O}$	0.4985	0.4645	0.3409
	$A_{\nu(Ti-O-Ti)}/ A_{\nu C=O}$	0.0792	0.1301	0.0992
	$A_{\delta(TiOH)}/ A_{\nu C=O}$	0.1014	0.0692	0.0405
	$A_{\nu(Ti-O-Ti)} / A_{\delta(TiOH)}$	0.78	1.88	2.45

Sample B: TTB=30wt%, room temperature, photocuring 6min
Sample C: TTB=30wt%, 90°C 80h, photocuring 6min
Sample D: TTB=30wt%, photocuring 1h

As can be seen from Fig 4 and Table 4, the relative content of OH($A_{\nu(OH)}/ A\nu_{C=O}$), as well as that of TiOH($A_{\delta(TiOH)}/ A\nu_{C=O}$) decreases with post-thermal treatment and photocuring time. However, the relative content of Ti O Ti group ($A_{Ti-O-Ti} / A\nu_{C=O}$), as well as the intensity ratio of TiOTi to TiOH ($A_{\delta(Ti-O-Ti)} / A_{\delta(TiOH)}$) increases under the same condition. As compared with sample B, the relative OH content of sample C decreases from 0.4985 to 0.4645, and TiOH content decreases from0.1014 to 0.0692. On the other hand, the relative content of TiOTi($A_{\nu(Ti-O-Ti)} / A_{\delta(TiOH)}$) increases ,from 0.78 to 1.88. It is worthy noting that exposure to UV light plays a much more significant role in the relative content of OH, TiOH and TiOTi than thermal treatment does. For sample D, the relative content of OH decreases from 0.4985 to 0.3409, and TiOH content decreases from 0.1014 to 0.0405. On the other hand, the relative content of TiOTi increases from 0.78 to 2.45 under the same condition.

In the case of photocuring for 1h, water could more easily vaporize from the hybrid film by thermal effect(>100°C) released from UV light during photopolymerization. Consequently, TiOH groups at the TiO_2 surface were brought in closer contact which allowed in turn to complete the condensation reaction to a greater extent than in the case of photocuring for 6min. Another possible reason was that when excessive water was added, in high humidity longer UV irradiation promoted hydroxyl groups to be effectively excited and break off , and form Ti-O-Ti bond [21,26], which were assumed to be ascribed to electronic processes stimulated by irradiation of photons.

According to the literature [27], FTIR spectroscopy is a reliable tool to determine the coordination mode of a carboxylate ligand in metal carboxylates. Indeed, the difference in frequency $\triangle \nu$ between antisymmetric and symmetric vibrations of C- O bonds has been usually related to the type of carboxylate coordination. Doeuff and Henry[28] considered that the coordinating complex of carboxylic acid could be predicted by $\triangle$v(v as - v s). Briefly, if $\triangle$v is lower than that

of free carboxylic ion, the coordination is chelate or bridging bidentate; otherwise, the coordination can be attributed to monodentate. Usually, the bridging structure gives rise to larger △ν between 140 and 160 cm^{-1} and the chelating structure a lower △ν between 80 and 92 cm^{-1}.

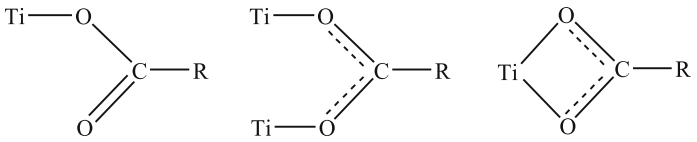

	Monodentate	Bridging bidentate	Chelating bidentate
$\nu a(COO^-)$	1720	1580	1550
$\nu s(COO^-)$	1295	1432	1463
$\Delta\nu = \nu a(COO^-) - \nu s(COO^-)$	425	148	87

Fig6 Possible carboxylate binding configurations of acetate ligands in Ti(IV)-acetate complexes

FTIR spectra of all samples are most informative in the low frequency carboxylic acid region. The IR stretches in the low frequency region, $\nu a(COO^-)$at 1580cm^{-1}, 1550cm^{-1} and $\nu s(COO^-)$at 1463cm^{-1} and 1432cm^{-1}, are indicative of ionic bonding between carboxylates and surface cations. The presence of two $\nu s(COO^-)$ modes suggests two COO^- binding configurations defined as chelating bidentate and bridging bidentate based on the νa-νs splitting magnitude(△ν ∼87cm^{-1} and 148cm^{-1}, respectively)(as shown in Fig6), This suggests that acrylic acid acts as a bidentate chelating coordination mode as well as a bidentate bridging coordination mode [29,30].

It is also noteworthy to look at the carbonyl stretch in the 1700cm^{-1} region. A carbonyl stretch will only be observed in the presence of free carboxylic acid or monodentate binding. No stretch at 1700 cm^{-1} is observed for all samples, an observation consistent with the analysis of the △ν splitting magnitude. These results suggest that acrylic acid completely reacts with titania alkoxide. Therefore the polymer chains are covalently bonded to the titania component.

3.4 AFM study

AFM can provide valuable information on nanoclusters and can serve as ideal tool to characterize cluster covered surfaces since a wide range of materials can be chosen as substrates for cluster deposition.

The bright and dark regions of AFM phase images, as shown in Fig 7-9, correspond to the inorganic domain and organic domain, respectively.

The AFM phase images show that the phase morphologies of the hybrid films are close correlated to the post- thermal treatment. The AFM micrographs of the hybrid films with and without post-thermal treatment show the presence of inorganic domains with mean size of 28.8nm, 25.3nm, respectively. This suggests that the inorganic domain sizes are related to the post- thermal treatment.

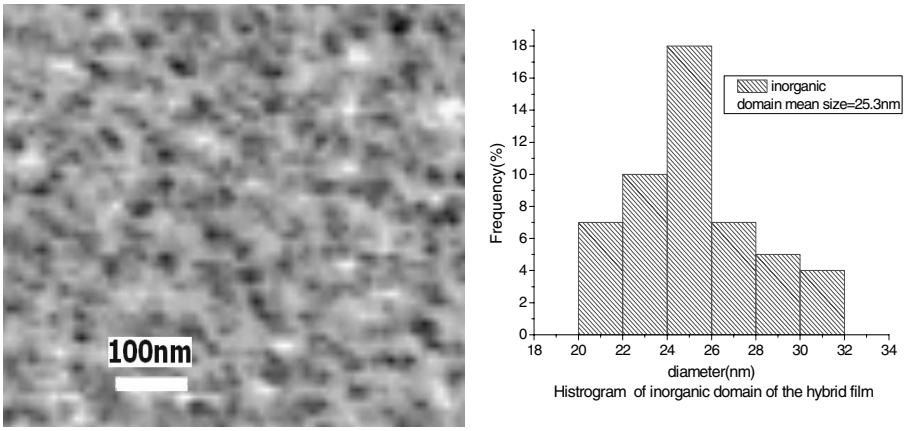

Fig 7 AFM phase diagram of the titania-acrylic polymer hybrid film: TTB=30wt%, non-post thermal treatment, photocuring 6min

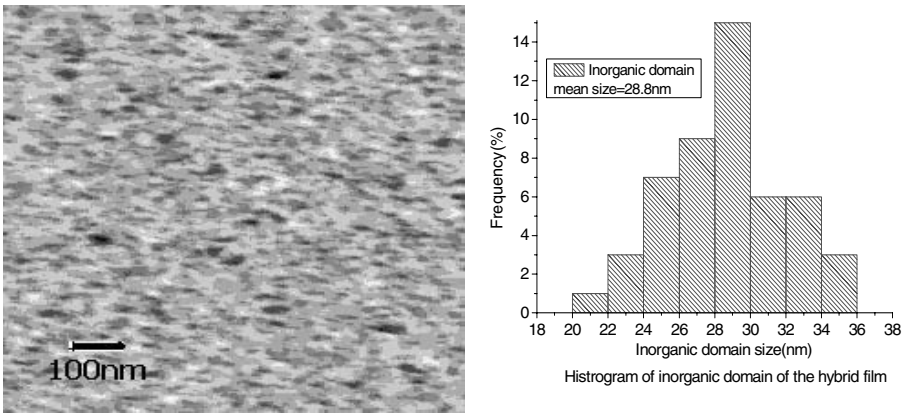

Fig 8 AFM phase diagram of TiO_2/polyacrylates film with post-heat treatment (TTB=30wt%, photocuring 6min, post-heat treatment: 90°C 80h)

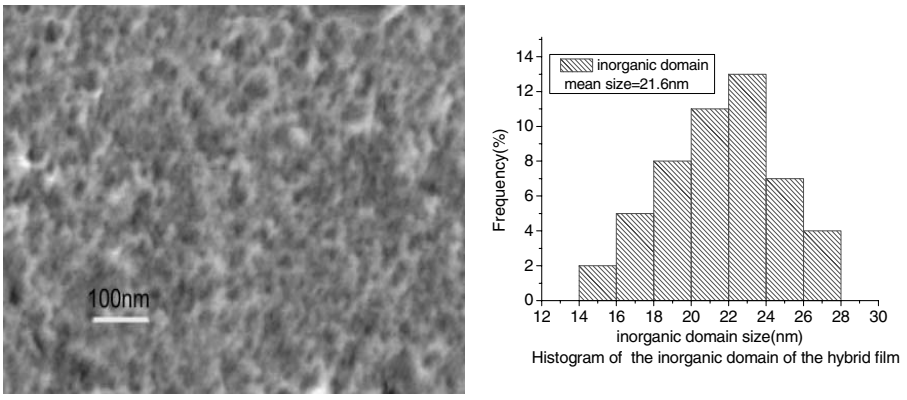

Fig 9 AFM phase diagram of TiO_2/polyacrylates film with photocuring 60min (TTB=30wt%)

The AFM phase image of samples with irradiation 6min as shown in Fig 7-8, indicated a noncontinuous inorganic domains entrapped by polymeric networks at a TTB fraction of 30wt%,and the inorganic phases were uniformly dispersed in the polymeric networks. However, the AFM phase image of sample with irradiation 60min, as shown in Fig 9, indicated a continuous inorganic domain formed at a TTB fraction of 30wt% This may be ascribed to particle aggregation caused by surfactant desorption from the TiO_2 particles as a result of the tremendous heat released from the infrared ray irradiation with 60min irradiation.

In conclusion, the AFM phase images showed the inorganic domains, with mean size of 21.6nm -28.8nm, were uniformly dispersed in the polymeric networks.

Above all, we have found that the synthesis of titania-polyacrylate nanocomposites by conventional sol-gel process result in precipitation with TTB content as high as 30wt% and the obtained hybrid materials were opaque. However on the same condition the obtained hybrid materials by sol-gel process in reverse micelles were transparent. So the effect of the reverse micelles on the hybrid morphology and structure was obvious, as indicated by AFM images. Therefore the new preparation method of the titania-acrylic polymer hybrid films by sol-gel methods in reverse micelles and in-situ photopolymerization was effective.

4. Conclusions

Nanosized titania –polyacrylate hybrid films have been produced by controlled hydrolysis of titanium tetrabutoxide (TTB) in Span85/Tweeen80 reverse micelles and subsequent in-situ photopolymerization. The titania-acrylic polymer films can upgrade the decomposition onset temperature as well as the temperature at which there is a maximum mass loss rate(T_{max}). Exposure to UV light and post-thermal treatment can decrease the T_{onset} and T_{peak} and increase the $\triangle H$ of the exothermal peak, and decrease the condensation temperature between TiOH. FTIR spectra suggest that acrylic acid acts as a bidentate coordination mode, indicative of chemical linkages between inorganic and organic phases. AFM images show that the hybrid films have characteristics of homogeneously distribution of the inorganic phases in a nanosized scale within the polymer matrix.

Acknowledgements

The authors gratefully acknowledge fruitful discussion with Professor Zhang Yong of Chengdu University of Technology on the preparation of nanosized TiO_2.They are also grateful to Yuan yi and He wen-qiong of Chengdu University of Technology, for extending all possible facilities.

References

1. Sreekumari P N, Radhakrishnan T, Revaprasadu N, *et al* (2005) *Applied Physics A: Materials Science & Processing* 81(4):835
2. Smirnova T, Sakhno O, Bezrodnyj V(2005) *J. Applied Physics B: Lasers & Optics* 80(8):947
3. Izaak T I, Babkina OV, Mokrousov GM (2005) *Technical Physics* 50(5):669
4. Bhimaraj P B, David LA, Gregory W, *et al* (2005) *Wear* 258(9):1437
5. Nad S, Sharma P, Roy I, *et al*(2003) *Journal of Colloid and Interface Science* 264(1): 89

6. Yoshida M, Prasad PN(1996) *Chem Mater* 8: 235
7. Hu Q, Marand E(1999) *Polymer* 40:4833
8. Wang B, Wilkes GL, Hedrick JC, *et al*(1991) *Macromolecules* 24: 3449
9. Lee L H, Chen WC(2001) *Chem Mater* 13:1137
10. Hiroyo S, Kanayo T, Yasuhiko A, *et al*(2004) *Thin Solid Films* 466: 48
11. Blanchard J, Doeuff SB, Maquet J, *et al*(1995) *New J. Chem* 19:929
12. Durand SP, Rouviere J, Guizard C(1995) *Coll Surf* 98:251
13. Ginzberg B, Bilmes S A (1996) *Progr Colloid Polym Sci* 102:51
14. Francois N, Ginzberg B, Bilmes S A(1998) *J Sol-Gel Sci Tech* 13:341
15. Schubert U, Lorenz NA(1995) *Chem Mater* 7:2010
16. Schubert U, Arpac E, Glaubitt WA, *et al*(1992) *Chem Mater* 4:291
17. Livage J (1997) *Act Chem*, 10: 4
18. PERRIN F X., NGUYEN V., VERNET J.L (2003) *Journal of Sol-Gel Science and Technology* 28: 205
19. Zhang R B, Gao L (2002) *Materials Research Bulletin* 37(9):1659
20. Yasushige M, Yasuhiro O ,Yuki T (2001) *Journal of Nanoparticle Research* 3: 219
21. Imai H, Morimoto H, Awazu K(1999) *Thin Solid Films* 351:91
22. Imai H, Morimoto H, Tominaga A, *et a*l(1997) *J Sol-Gel Sci Technol* 10:45
23. C.C. Perry, X. Li, and D.N. Waters (1991) *Spectrochimica Acta* 47:1487
24. Pirson A., Mohsine A, Marchot P, *et al*.(1995) J. Sol-Gel Sci. Tech. 4:179
25. DJAOUED Y., BADILESCU S, ASHRIT P.V(2002) J*ournal of Sol-Gel Science and Technology* 24: 247
26. Hirai S, Shimakage K, Sekiguchi M(1999) *J Am Ceram Soc* 82:2011
27. Mehrotra R.C, Bohra R *Metal Carboxylates* (Academic Press, London, 1983), p. 48
28. Doeuff S, Henry M, Sanchez C, Livage J(1987) *J. Non-Cryst Solids* 8: 206
29. Dunuwila DD, Gagliardi D, Berglund KA(1994) *Chem. Mater* 6:1556
30. Yasumori A, Ishizu K, Hayashi S, Okada K(1998) *J Mater.Chem* 8:2521